SF2A 2015
F. Martins, S. Boissier, V. Buat, L. Cambrésy and P. Petit (eds)

IMPACT OF THE QPO MODELS ON THE PULSE PROFILE

P. Varniere[1] and F. H. Vincent[2]

Abstract. Quasi-periodic oscillations (QPO) are an important probe of the timing properties of black-hole binaries. Many models are proposed in order to account for these features and it is difficult to differentiate them with current data. Here we aim to look at the actual pulse profile from each model in order to see how they could be differentiated and what kind of sources are the best targets for such a test. We consider three classes of simple models: elongated hot spots, tori and spirals. We perturb the equilibrium temperature of a thin disk to create these structures. The perturbed disk is supposed to emit blackbody radiation at the local temperature. Radiation is ray-traced in the Schwarzschild metric to a distant observer. We study the dependency with the source inclination of the pulse profile for different frequencies for these three models. The departure from a pure sinusoid of certain models at high inclination will be visible in the power density spectra by a higher presence of harmonics. In particular, hot spots and spirals lead to a (complete or partial) harmonic series which is lacking for a radially oscillating tori. We conclude that analyzing the first harmonics of the dominant power density spectrum peak for high-inclination sources is an interesting probe and it might make it possible to differentiate between axisymmetric (tori) and non-axisymmetric (hotspots and spirals) models.

Keywords: black hole, QPO, general realtivity

1 Introduction

Up to now QPO models have been focusing mainly on explaining the frequency (or frequencies) observed in the power density spectrum (PDS). While it is essential, it is just the first accessible observable and all of the models fulfilled this requirement as they were created for it. It is therefore interesting to take those same models and look at how they compare for other observables. Some we already have as the root mean square (rms) amplitude, some we do not yet have complete access to such as the pulse profile. This will allow us to see what would be necessary to differentiate between the models, in particular in the context of the next generation of instruments, but also what are the best candidate observables with present data.

2 From the disk emission to the Pulse profile

2.1 Simple model for the temperature profile

QPO models often connect the signal modulations to the presence of structures embedded in the disk. Such structures include axisymmetric (see e.g. Bursa *et al.* 2004; Schnittman *et al.* 2006b; Vincent *et al.* 2014), or precessing (Schnittman *et al.* 2006c; Ingram *et al.* 2009) tori, hotspots (Karas *et al.* 1992; Schnittman & Bertschinger 2004; Tagger & Varniere 2006; Pechacek *et al.* 2013) and spirals (Tagger & Pellat 1999; Varniere *et al.* 2002; Varniere & Blackman 2005; Karas *et al.* 2007).

Our main concern here is not the origin of the structure, but the consequences on the emission. This means that, rather than taking full magnetohydrodynamic (MHD) simulations of the different models proposed to explain QPOs we are interested in, we decided to create a simple, analytical, model for the different structures in order to test more cleanly the different parameters. Indeed, in a full fluid simulation changing one parameter

[1] AstroParticule & Cosmologie (APC), UMR 7164, Universit Paris Diderot, 10 rue Alice Domon et Leonie Duquet, 75205 Paris Cedex 13, France.
[2] LESIA, CNRS UMR 8109, Observatoire de Paris, Universite Pierre et Marie Curie, Universite Paris Diderot, 92190 Meudon, France

in the initial condition can have repercussions on several observable parameters and therefore it is harder to study the different effects separately.

We take a pertubative approach to the disk temperature profile by adding to the disk hydrostatic equilibrium temperature $T_0(r) \propto r^{-1}$ a component that depends on time, radius and azimuthal angle $T_1(t, r, \varphi) = T_0(r)d(r)\, s(r - r_s, \varphi)$. This allows us to minimize the number of parameters to characterize the structures in the disk while keeping a similar framework. The quantity $r_s = r_s(t, \varphi)$ represents the structure added to the equilibrium disk in time-dependent polar coordinates, it can either be a torus, a hotspot or a spiral. We choose to decompose T_1 as a height function d that depends only on r and a shape function s which is finite only near the disc structure we are studying. This allows us to keep the same structure to take into account a variety of shapes mimicking a variety of models. For simplicity we take the shape function to be gaussian and the height function to be a power-law of r only and related to the equilibrium temperature $T_0(r)$. This provides a simple but useful framework to model a disk with added perturbative structures. Within this framework the perturbed temperature reads

$$T(t, r, \varphi) \quad = \quad T_0(r) \times \left[1 + \gamma \left(\frac{r_c(t)}{r}\right)^{\beta} \exp\left(-\frac{1}{2}\left(\frac{r - r_s(t, \varphi)}{\delta}\right)^2\right)\right] \tag{2.1}$$

where $r_c(t)$ is the position of the temperature maximum in the disk (the center of the torus or hotspot). This quantity is allowed to be a function of time. The quantity β measures how fast the temperature decreases from the maximum at r_c, δ parametrizes the radial extent of the structure while γ is the maximum amplitude of the perturbation.

2.2 *The general relativistic ray-tracing code GYOTO*

In order to simulate the observed light-curve, we use the open-source general relativistic ray-tracing code GYOTO (Vincent *et al.* 2011). We assume the structure to be at rest in a reference frame corotating with the disk at the Keplerian velocity at radius r_c. Null geodesics are integrated backward in time from a distant observer to the disk. When the disk is hit, the outgoing flux is assumed to follow the blackbody law at the local temperature. We are using the (*Schwarzschild* or *full-GR* case in the following) taking into account the Schwarzschild metric, thus all special and general relativistic effects for a non-rotating black hole.

3 Modulation from an axi-symetrical torus

The first model we study is the resulting flux modulation coming from the radial oscillation of a torus. The position of the torus is defined bt $r_c(t) = r_{c,o}(1 + A\sin(\Omega(r_{c,o})\sqrt{1 - r_{LSO}/r_{c,o}}t))$. Here we choose the amplitude of the oscillation $A = 0.1$. This corresponds to adding to a non- oscillating torus a velocity perturbation of the order of a few percent of the local Keplerian velocity, so this is a rather big oscillation, but the dominating motion is of course still azimuthal.

On the right of Fig. 1. we show the lightcurves at inclination 20° in the case of a torus positioned at $r_c \in \{2, 3, 4, 6, 8\}r_{LSO}$ while the other parameters are identical. The shape of the lightcurve stays consistent with a higher amplitude sinusoid while keeping the mean value at the same phase location. The increase in the rms amplitude is to be expected, indeed the amplitude of the torus oscillation is about 10% of its average position, therefore when the torus is further away in the disk the variation in position also increases thus causing a stronger modulation.

On the left of Fig. 1. we show the same lightcurves but this time seen at a high inclination of 70°. Similarly to what we saw at low inclination the shape of the lightcurves stay consistent with a sinusoid whose amplitude increased as the structure gets further away in the disk.

Observationally, this would mean that, while the rms amplitude of the QPO increase with inclinations, the pulse shape is unaffected and the PDS would not show variation on the harmonic content between high and low inclination systems.

4 Modulation from non axi-symetrical structure: an elongated blob or spiral

A lot of QPO models imply the presence of a non axi-symetrical structure in the disk. Here we take two of those structures to see how the pulse profile and hence the PDS would behave as a function of distance and

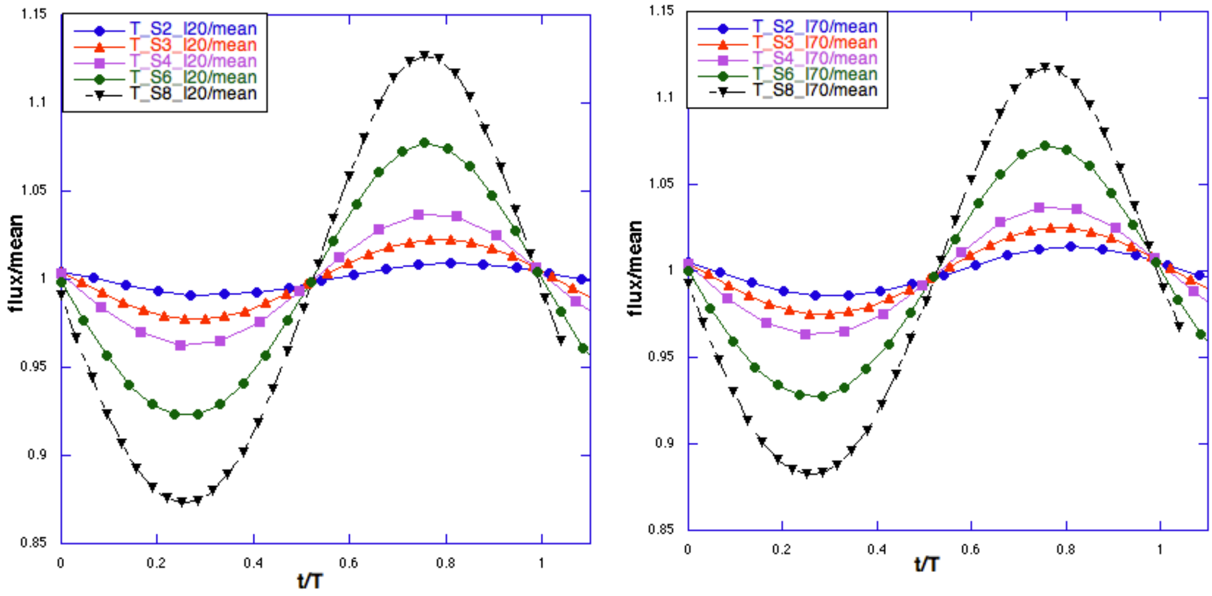

Fig. 1. Comparison of one period of the light curves obtained in the case of a torus at different positions in the disk. The legend of the graph shows T for a torus, S followed by a number represent r_c and I is for the inclination. **Left:** Case of a 20° inclination. **Right:** Case of a 70° inclination. All of them are sinusoidal for both inclination.

inclination.

First, we look at the case of a large, heavily sheared, hotspot of azimuthal extend $\delta\varphi = \pi$, this is a final stage of any blob that is not sustained by any instability, indeed shear will tend to circularize any overdensity. We see on the left if Fig. 2 that having the position of the blob further away in the disk also has no detectable effect of the shape of the light curve. Still, there is a very small departure from a pure sinusoide that gets

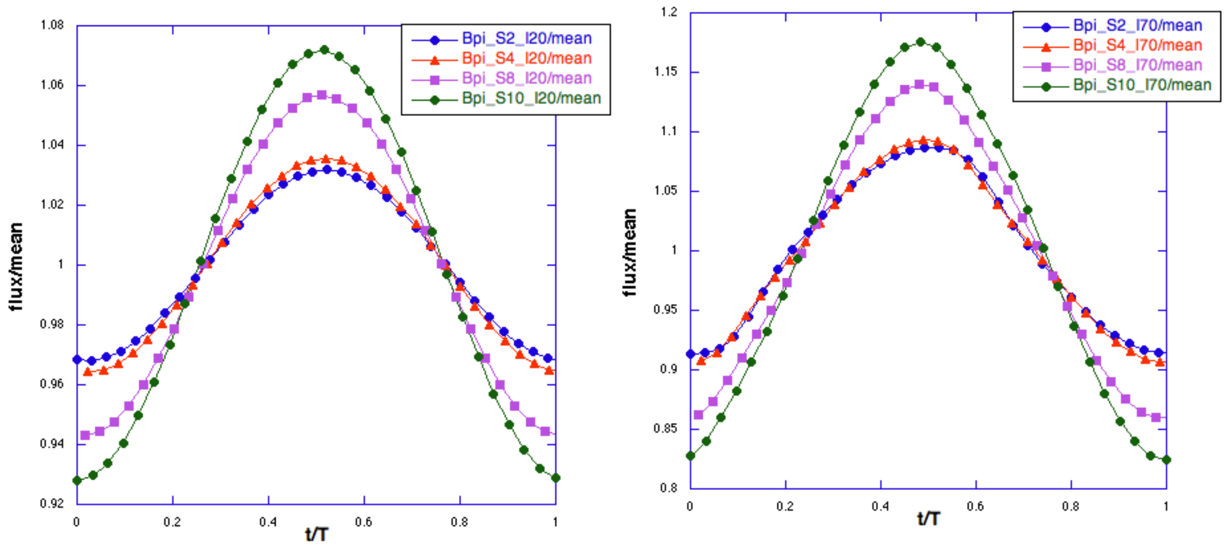

Fig. 2. Comparison of one period of the light curves obtained in the case of an elongated blob at different positions in the disk. **Left:** Case of a 20° inclination. **Right:** Case of a 70° inclination. A slight departure from a pure sinusoide is visible at high inclination, seemingly more visible for structures further away in the disk.

stronger as the structure moves further away in the disk (this is well below 1% of the rms of the main peak even at $r_c = 10$ thus not detectable among the noise). Similarly as in the torus case, the rms amplitude increases with the radius of the structure, though it is not as pronounced in the case of the blob. Indeed, the increase in rms comes from the fact that, while changing r_c, we keep the ratio r_c to the inner edge of the disk constant, hence reducing the average, unmodulated, flux.

When we look at the system from a higher inclination, as we can see on the right of Fig. 2, there is a clear departure from a sinusoide that gets stronger as the blob is further away in the disk. Such a change in the pulse shape will have an strong impact when looking at the PDS. From looking at just the torus and the hotspot cases we see that, while providing the required increase in rms with inclination, the pulse profile from those two models differ widely between low inclination and high inclination systems. This will have detectable consequences on the PDS as one will have a higher harmonic content for a high inclination system than for a low one, while there is no change for the radially oscillating torus.

Just as excepted from the similitude of their modulation mechanism, we see on Fig. 3. a similar trend for the case of a one-arm spiral perturbing the disk. Once again the lightcurve has a slight, barely visible, departure from a sinusoide and when looking at Fourier space a small first harmonic might be detected, especially when the spiral is further out in the disk.

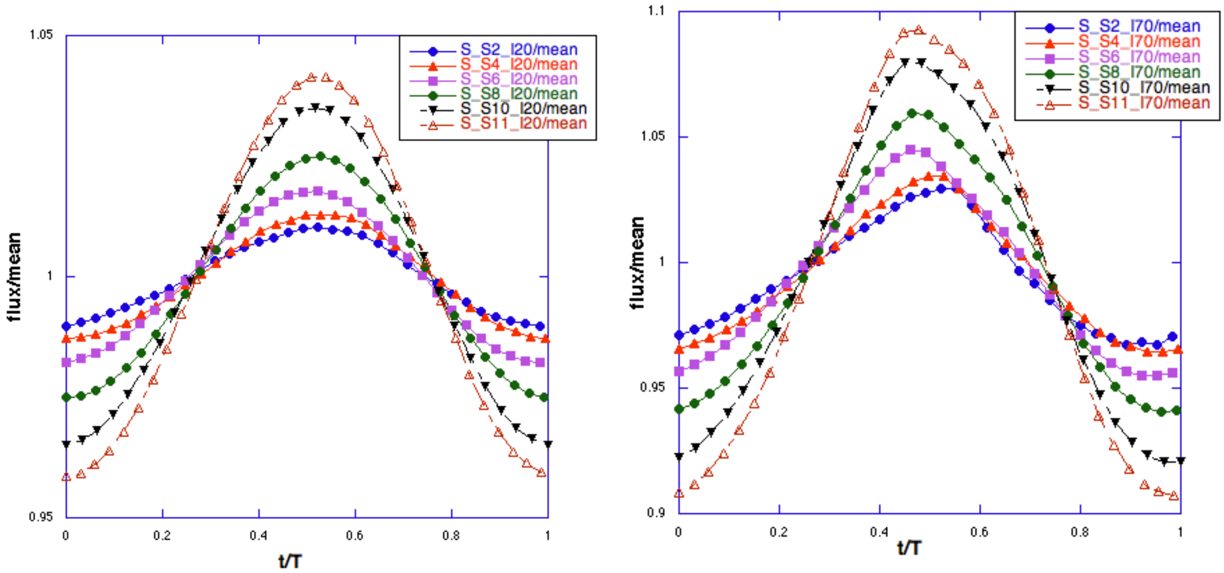

Fig. 3. Comparison of one period of the light curves obtained in the case of a spiral at different positions in the disk. **Left:** Case of a 20° inclination. **Right:** Case of a 70° inclination. There is a definite departure from a sinusoide at high inclination, seemingly increasing for structures further away in the disk.

This is even more visible at higher inclinations as shown on the right of Fig. 3. As in the case of the hotspot the shape of the pulse is strongly affected by the inclination.

The main difference with Fig. 2 is in the detailed shape of the pulse which is clearly not symmetrical with respect to the average value for the spiral, meaning the time spent at higher flux than the mean value will be shorter than the time spent at lower flux. While this is hardly detectable now, we might find some high inclinations system having a strong QPO in which we can try to assess the time spent above and below the mean value.

5 Conclusions

Here we have computed and compared the pulse profile of three QPO models. From this, it seems that the only axi-symmetrical model we studied, a simple radially oscillating torus, would be distinguishable from the other, non-axi-symmetrical, models by the lack of change in its harmonic contents between high and low inclination systems. It is therefore interesting to start looking at the harmonic content of sources at different inclinations to see if a statistically significant change with inclination is detected.

Distinguishing between the different non-axi-symmetrical models would be more difficult and would require finding stable high inclination systems with strong QPOs in which we could compare the difference between the average and the mean of the light curve. This might be feasible with the next generation of X-ray missions.

PV acknowledges financial support from the French Programme National des Hautes Energies (PNHE) and the UnivEarthS Labex program at Sorbonne Paris Cite (ANR-10-LABX- 0023 and ANR-11-IDEX-0005-02). Computing was done at the FACe (Francois Arago Centre) in Paris. FHV acknowledges financial support from the Polish NCN grant 2013/09/B/ST9/00060.

References

Bursa M., Abramowicz M. A., Karas V., Kluzniak W., 2004, The Astrophysical Journal Letter, 617, L45

Feroci, M., et al., 2014, Proceedings of the SPIE, 9144, 2

Ingram, A., Done, C., Fragile, P. C., MNRAS, 397, L101

Karas, V., Vokrouhlicky, D., Polnarev, A. G., 1992, MNRAS, 259, 569

Karas, V., Dovciak, M., Eckart, A., Meyer, L., 2007, Proceedings of RAGtime 8/9

Pechacek, T., Goosmann, R. W., Karas, V., Czerny, B., Dovciak, M., 2013, A&A, 556, A77

Schnittman J. D., Bertschinger E., 2004, The Astrophysical Journal, 606, 1098

Schnittman J. D., Rezzolla L., 2006, The Astrophysical Journal Letter, 637, L113.

Schnittman, J. D., Homan, J., Miller, J. M., 2004, ApJ, 642, 420

2002, ApJ, 564, 962.

Tagger, M. & Pellat, R., 1999, 349, 1003.

Tagger, M. & Varniere, P., 2006, ApJ, 652, 1457.

Varniere, P. & Blackman, E.G., 2005, New Astronomy, Volume 11, Issue 1, p. 43.

Varniere, P.; Rodriguez, J.; Tagger, M., 2002, A&A, 387, 497.

Varniere, P. & Mignon-Risse, R., 2016, to be submitted A&A.

Varniere, P. & Mignon-Risse, R., 2015, proceeding de la SF2A.

Vincent, F. H., Paumard, T., Gourgoulhon, E., & Perrin, G. 2011, Classical and Quantum Gravity, 28, 225011.

Vincent, F. H.; Mazur, G. P.; Straub, O.; Abramowicz, M. A.; Kluzniak, W.; Torok, G.; Bakala, P., 2014, A&A, 563, A109.